**PRIMARY REVERSE OXYGEN-ISOTOPE EVOLUTION OF PYROXENE IN COMPACT TYPE A CAIs FROM THE EFREMOVKA AND NWA-3118 CV3 CHONDRITES: INSIGHTS INTO INTERNAL CAI MIXING LINES.** G. J. MacPherson[1], K. Nagashima[2], M. A. Ivanova[1], and A. N. Krot[2] . [1]US National Museum of Natural History, Smithsonian Institution, Washington, D.C., 20560 USA. E-mail: macphers@si.edu. [2]Hawai'i Institute of Geophysics and Planetology, University of Hawai'i at Manoa, Honolulu, HI 96822 USA.

**Introduction:** One general characteristic of primary igneous pyroxene (and spinel) in coarse-grained Ca-Al-rich inclusions (CAIs) from CV3 chondrites is an $^{16}$O-rich isotopic signature, whereas melilite and anorthite in the same CAIs are both $^{16}$O-depleted to varying degrees [1]. This isotopic dichotomy is commonly interpreted to reflect secondary isotopic exchange in the solid state, because anorthite and melilite have higher oxygen diffusion rates than do pyroxene or spinel. Yet despite its widespread acceptance, this model is problematic because in detail the observed isotopic fractionation between minerals do not completely agree with expectations from measured diffusion coefficients. [2]. One particular problem is that clinopyroxene should better preserve the $^{16}$O-rich isotopic signature than spinel, yet the opposite is commonly observed. For this reason [1] advocated a complex exchange model with multiple melting and exchange events.

**Analytical procedures:** Polished thick sections of 4 compact Type A CAIs from the Efremovka (*20bE*) and NWA-3118 (*1N-B, 9bN, 16N*) CV3 chondrites were characterized prior to SIMS analysis, using both a scanning electron microscope and electron microprobe. All isotopic analyses were acquired using the Cameca IMS-1280 at the University of Hawaii, operated under conditions similar to those described in [3] and using a ~7×7 μm rastered beam spot.

**Results:** Inclusion *1N-B* is a ~2 cm diameter, round torus-shaped inclusion, with the central hole being filled by meteorite matrix. A Wark-Lovering (WL) rim sequence covers both the exterior and interior (of the torus) surfaces. The CAI consists mostly of melilite, with greatly subordinate spinel, equant euhedral pyroxene ("fassaite"), and scattered perovskite grains enclosed in pyroxene, spinel, and melilite. The pyroxene is strongly zoned, with Ti-Al-rich interiors and diopsidic rims. Overall this CAI appears to have experienced a major degree of partial melting. Spinel is uniformly $^{16}$O-rich (Fig. 1a), melilite is mostly $^{16}$O-poor, but the pyroxene is so heterogeneous isotopically ($\Delta^{17}$O = -3‰ – -23‰). that it covers most of the entire range of the CCAM line. The pyroxene crystals are isotopically zoned, with the Ti-Al-rich interiors being $^{16}$O-poor and the diopsidic rims being $^{16}$O-rich (Fig. 2); *i.e.*, the crystals evolved down – not up – the CCAM line. Ti-Al-rich pyroxene in the WL rim is also $^{16}$O-depleted. Inclusion *20bE* is a small (~2.7 mm in apparent diameter) oblong CAI fragment on which the Wark-Lovering rim covers only about half of the exposed CAI area. The CAI consists mostly of melilite, with a minor amount of spinel on one side of the inclusion and a few large (up to ~0.5 mm) pyroxene crystals in the center of the inclusion. Spinel in *20bE* is uniformly $^{16}$O-rich (Fig. 1b) and melilite is mostly $^{16}$O-poor. The pyroxene is more homogeneously $^{16}$O-rich than that in *1N-B*, but nevertheless does exhibit a distinct range in isotopic composition ($\Delta^{17}$O = -21‰ – -24‰). Inclusion *9bN* is a compact but somewhat irregularly-shaped CAI, ~1.2 cm in maximum dimension. The mineralogy again is melilite plus minor pyroxene and spinel, but in this object the pyroxene occurs as clearly interstitial grains to the melilite; many having arcuate shapes and all are mantled by Mg-rich melilite, suggestive of the merest beginnings of partial melting (cf. *1N-B*). The WL rim sequence of this CAI is dominated by tiny blades of hibonite that are far more abundant than even spinel. Isotopically *9bN* resembles *20bE* in nearly all respects (Fig. 1c), with $^{16}$O-rich spinel, $^{16}$O-depleted melilite, and pyroxene that is $^{16}$O-enriched but with a clear range in compositions ($\Delta^{17}$O = -18‰ – -24‰). Only a ~8 mm portion of CAI *16N* is contained within the thin section so the original size was greater than that. Melilite is the dominant phase, but pyroxene and spinel are both relatively abundant compared with the other CAIs in this study. 16N is distinctive also in containing irregular grains of interstitial anorthite in the interior, and numerous small perovskites generally enclosed within pyroxene. Had this inclusion melted more thoroughly, it would appear transitional to a Type B. This CAI is similar isotopically to *1N-B*: the pyroxene covers almost the entire span of the CCAM line ($\Delta^{17}$O = -3‰ – -22‰). Ti-Al-rich pyroxene in the WL rim is also $^{16}$O-rich ($\Delta^{17}$O = -22‰ – -23‰). Melilite is uniformly $^{16}$O-poor, spinel is $^{16}$O-rich, and anorthite is more $^{16}$O-enriched than melilite. Perovskite is the most $^{16}$O-poor phase of all, plotting just below the terrestrial fractionation line ($\Delta^{17}$O = -2‰).

**Discussion.** The isotopic compositions of the pyroxenes in these Type A CAIs are clearly correlated with pyroxene bulk composition, and moreover are opposite of what would normally be expected – isotopically heavy in the crystal interiors and $^{16}$O-rich on the crystal rims. This clearly is a crystal growth phenomenon and has nothing to do with solid state

diffusion during later isotopic exchange. The answer to the problem lies in the observed isotopic compositions of perovskites in these and other Type A CAIs [e.g. 4], and the observation that pyroxene commonly encloses perovskite. Perovskite apparently exchanges oxygen even more easily than does melilite, and from the textures we infer that the pyroxene initially forms by reaction of perovskite with melilite. This reaction, possibly due to the onset of partial melting, occurred after perovskite exchanged its oxygen isotopes but prior to melilite doing so. Thus the pyroxene crystals initially formed with a $^{16}$O-depleted composition inherited from the perovskite, and became progressively more $^{16}$O-rich as the melilite isotopic reservoir begins to dominate. Only subsequent to this process did the melilite itself exchange. Ryerson and McKeegan [2] noted the unexpected isotopic composition of pyroxene in Type B CAIs relative to coexisting phases and their respective diffusion coefficients, with the pyroxene commonly being less $^{16}$O-rich than the coexisting spinel and exhibiting a range of compositions. For this reason [2] rejected a simple solid-state exchange model to explain the isotopic mineral compositions within Type B CAIs. Our observations suggest that the apparent anomalous compositions of the pyroxene may be inherited from the earliest stages of CAI melting, when their isotopic compositions were initially imposed by the perovskites they formed from. Thus the internal isotopic mixing lines of individual Types B and A CAIs do reflect both complex CAI histories and solid-state exchange, as suggested by [2] albeit in a somewhat different way than envisioned by them. Our observations also require that the $^{16}$O-poor reservoir existed very early in the solar nebula, albeit locally, contemporaneous with the $^{16}$O-rich reservoir and with formation of CAIs.

**References:** [1] Yurimoto H. et al. (2008) In *Oxygen In The Solar System . Rev. in Mineralogy and Geochemistry* **v. 68**, 141. Min. Soc. Am. Spec. Paper. [2] Ryerson F. J. and McKeegan K. D. (1994) *GCA*, **17**, 3713-3734. [3] Makide K. et al., (2009) *GCA* **73**, 5018-5050 [4] MacPherson G.J. et al. (2010) *MAPS* 45 Suppl., A125 (abstr. #5267).

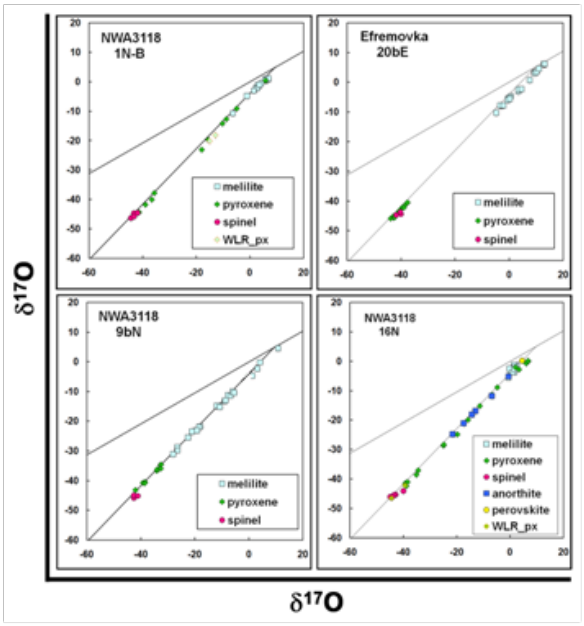


*Fig 1. Oxygen isotopic compositions of four CAIs.*

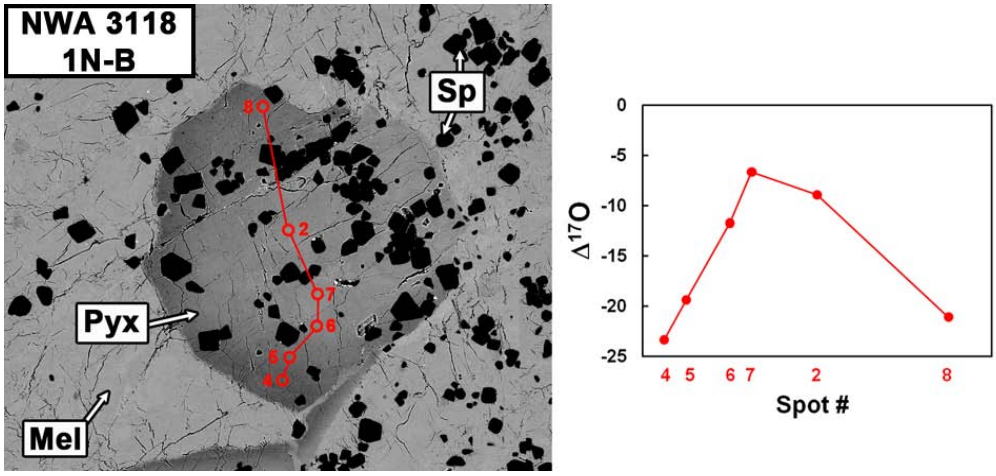


*Fig 2. BSE image (left) and O-isotopic profile (right) of a zoned pyroxene crystal in CAI NWA 3118 1N-B. The darker pyroxene rim is Al-Ti-poor and $^{16}$O-rich relative to the crystal interior*